Nanoscale Research Letters
a SpringerOpen Journal

NANO EXPRESS   **Open Access**

Thermally modulated biomolecule transport through nanoconfined channels

Lei Liu[1,2*] and Lizhong Zhu[1]

Abstract

In this work, a nanofluidic device containing both a feed cell and a permeation cell linked by nanopore arrays has been fabricated, which is employed to investigate thermally controlled biomolecular transporting properties through confined nanochannels. The ionic currents modulated by the translocations of goat antibody to human immunoglobulin G (IgG) or bovine serum albumin (BSA) are recorded and analyzed. The results suggest that the modulation effect decreases with the electrolyte concentration increasing, while the effects generated by IgG translocation are more significant than that generated by BSA translocation. More importantly, there is a maximum decreasing value in each modulated current curve with biomolecule concentration increasing for thermally induced intermolecular collision. Furthermore, the turning point for the maximum shifts to lower biomolecule concentrations with the system temperature rising (from 4°C to 45°C), and it is mainly determined by the temperature in the feed cell if the temperature difference exists in the two separated cells. These findings are expected to be valuable for the future design of novel sensing device based on nanopore and/or nanopore arrays.

Keywords: Nanopore arrays; Biosensing; Transporting property

Background

In the past years, nanopore-based device is attracting more and more attentions for its potential applications in selective molecular separation [1,2], biosensing [3,4], energy storage [5,6], controlled release [7,8], drug delivery [9,10], nanofluidics, and nanoelectronics [11-14]. It is generally believed that the premise of this method is how to obtain proper nanopores and how to design effective fluidic device. Till now, natural nanopores in biomembranes [15,16] and artificial nanopores in inorganic films [17-19] are two major types of pores used in this area, while nanopores in polymer membranes obtained by track-etching method also can provide other possible choices [20-23]. Since the transport of mass and charge in the confined nanochannels, novel phenomena which cannot be observed in the bulk solutions will occur [24-26]. As we known, the flow of water and the molecular mobility in confined spaces is much faster

than that in bulk case [27-29]. These phenomena indicate that the controlled transport of mass and charge through confined spaces is a fundamental process of interest in biology, physics, and chemistry, which have been regarded as an emerging field with major impact on bioanalysis and fundamental understanding of nanoscale interactions down to single molecule level [30-32]. Therefore, molecule or ion transport through nanopores is a key scientific issue for the fundamental understandings of the physical nature of analyte translocation. Although many important progresses have been established in this area, bridging theoretical calculations and experimental results conformably and ending up with an in-depth understanding of all problems is not an easy task. In this work, nanopore array-based sensing device has been fabricated by using PC ultrafiltration membrane, which is employed to investigate the thermally controlled biomolecular transporting properties in confined nanochannels.

Methods

Goat antibody to human immunoglobulin G (IgG) and bovine serum albumin (BSA) (bought from Nanjing Boquan Technology Co., Ltd., Nanjing, China) were

* Correspondence: liulei@seu.edu.cn
[1]Jiangsu Key Laboratory for Design and Manufacture of Micro-Nano Biomedical Instruments, School of Mechanics, Southeast University, Si Pai Lou 2#, Nanjing 210096, People's Republic of China
[2]Suzhou Key Laboratory for Design and Manufacture of Micro-Nano Biomedical Instruments, Suzhou Research Institute of Southeast University, Linquan street 399#, Suzhou 215123, People's Republic of China

Springer

used as analytes. KCl (analytical grade) solutions were employed as electrolyte. As illustrated in Figure 1a, nanofluidic device was made up of two separated cells linked by a chip containing nanopore arrays (pore diameter: 50 nm used for IgG and 15 nm used for BSA, the AFM characterization for 50-nm pore is shown in Figure 1b). The temperature in the feed cell and the permeation cell were controlled at 4°C, 22°C, and 45°C. The transmembrane ionic current under the applied voltage of 2.5 V was measured by Keithley 2000 multimeter (Keithley Instruments, Inc., Cleveland, OH, USA).

Obviously, ions (K^+ and Cl^-) in the solution moved directionally through nanopores result in the basic ionic current (I_0), while IgG or BSA molecules driven to pass through nanopores generate the modulated ionic currents (I). Generally, the change in the ionic current will be mainly affected by biomolecules' translocation. Once or BSA molecules enter nanopores, the volumes in the nanopores are partially occupied, which will prevent certain amounts of K^+ and Cl^- from passing through the confined channel, which will decrease the background ionic current (I_0). At the same time, the surface charge of IgG molecule will also contribute to the increase of the total ionic current when it passes through nanopore. The final current changes will be determined by the combined effects. Generally, the modulated ionic current (I) is smaller than the basic ionic current (I_0) if the concentration of the electrolyte solution is not too low. So the relative changing tendency of the modulated current can be reflected by the

value of $(I_0 - I)/I_0$. Figure 2a,b shows the values of $(I_0 - I)/I_0$ modulated by IgG and BSA in the electrolyte concentration of 0.01 and 1.00 mol/L, respectively, which are obtained at 4°C, 22°C, and 45°C. Comparing Figure 2a,b the modulated effects generated by biomolecules' translocation decrease with the electrolyte concentration increasing because of the background ionic current increasing, and the modulated effects caused by IgG (stocks diameter: 25 nm) are more significant than those caused by BSA (stocks diameter: 3.5 nm). More importantly, there exists a maximum decreasing value in each curve, which means the biggest place holding effect by biomolecules. The turning point concentration values corresponding to the maximum for IgG are 80 ng/mL (4°C), 40 ng/mL (22°C), and 20 ng/mL (45°C), respectively. Those values for BSA are 100 ng/mL (4°C), 40 ng/mL (22°C), and 20 ng/mL (45°C), respectively. Although there are slight differences in the detailed value for BSA and IgG, the changing tendencies for the two biomolecules are similar. It should be pointed out that the turning point for the modulated current curve with biomolecule concentration is the same with the turning point of biomolecule concentration corresponding to the maximum value of $(I_0 - I)/I_0$ for each case in our experiments.

Results and discussion

Figure 3 illustrates a single biomolecule (red ball) near a nanopore, and its sweeping volume in a period of time (δt) can be expressed as $\pi d^2 v \delta t$ (v: velocity which containing
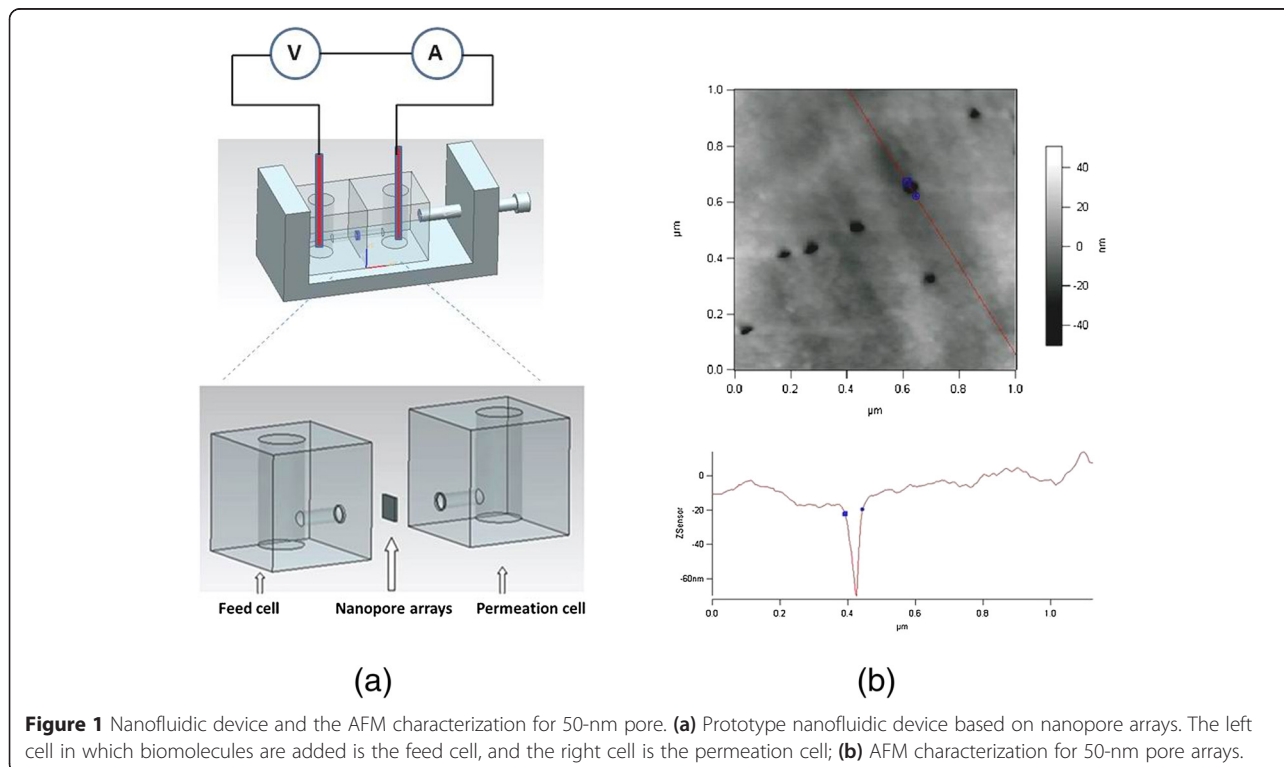

Figure 1 Nanofluidic device and the AFM characterization for 50-nm pore. **(a)** Prototype nanofluidic device based on nanopore arrays. The left cell in which biomolecules are added is the feed cell, and the right cell is the permeation cell; **(b)** AFM characterization for 50-nm pore arrays.
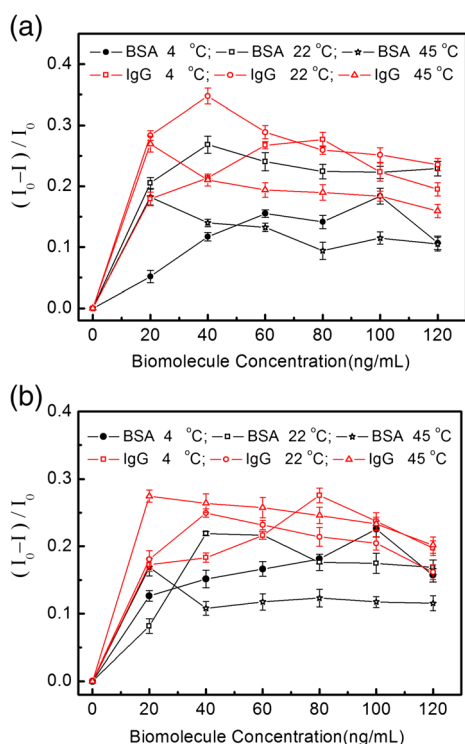
Figure 2 The value of $(I_0 - I)/I_0$ modulated by IgG and BSA in 0.01 mol/L (a) and 1.0 mol/L (b) KCl solution. The temperatures are controlled at 4°C, 22°C, and 45°C, respectively. $(I_0 - I)/I_0$ is defined as the relative variance ratio reflected the modulated current changing tendency, where I_0 and I stand for the ionic current without and with biomolecules modulation.

the axial velocity v_1 and the velocities in the other two mutually perpendicular directions represented as v_2 and v_3; d: stocks diameter of biomolecules). Its total number of collisions (Z) with other biomolecules in unit time can be expressed as $Z = \pi d^2 v n$ (n: number of other biomolecules in unit volume). Obviously, v_2 and v_3 contribute little to the biomolecule translocation. For an upcoming captured biomolecule near nanopore, keeping the speed of v_1 and continuing to move toward nanopore means translocation, while collisions will reduce its probability of translocation. Therefore, the increasing biomolecule concentration corresponds to the bigger number of molecules with potential translocation; while more biomolecules will gather near nanopores, the total number of collisions will also increase. The former raises the translocation probability, and the latter decreases the capture probability. Under the joint influences, there must exists a maximum value for IgG translocation with its concentration increasing.

As we known, temperature increasing means the larger internal energy, which can result in bigger moving intensity of biomolecules and ions. For one single biomolecule in the solution, its kinetic energy can be described as:

$$E = E_V + E_T = \frac{1}{2}mv^2 = \frac{1}{2}mv_1^2 + \frac{3}{2}K_BT \qquad (1)$$

in which $\frac{1}{2}mv_1^2$ is mainly determined by electric field and $\frac{3}{2}K_BT$ is determined by temperature. Based on Equation (1),
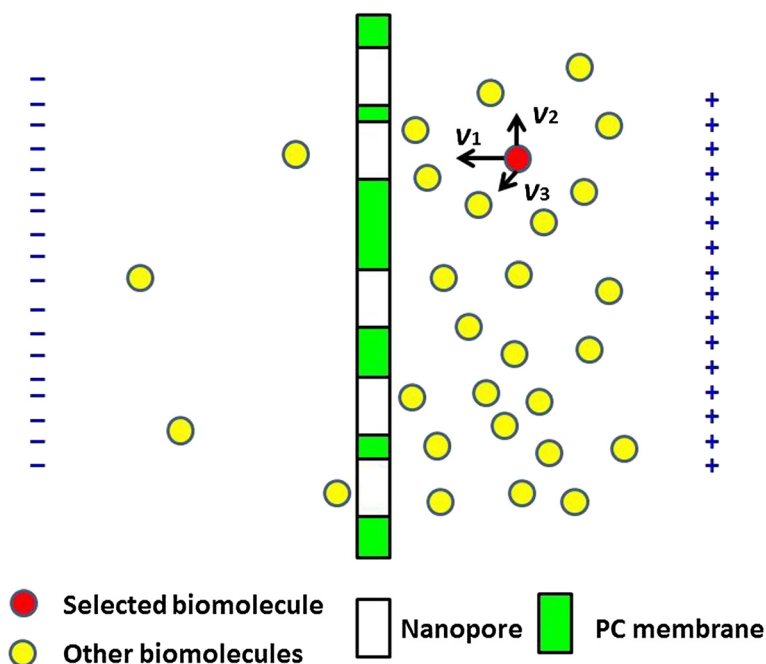

Figure 3 Schematic picture of a single biomolecule passing through nanopore arrays.

the total number of collisions (Z) in unit time can be rewritten as:

$$Z = \pi d^2 n \sqrt{v_1^2 + \frac{3K_B T}{m}} \qquad (2)$$

Furthermore, pH value of the solution will decrease slightly with the temperature rising. In our experiment, pH value decreases from 7.35 to 6.75 when the temperature increases from 4°C to 45°C. These changes in pH value can increase the charged amounts of biomolecule; therefore, higher temperature will result in bigger v_1 under the same accelerating voltage. With temperature increasing, more biomolecules will aggregate near nanopores, and at the same time, the total number of collisions (Z) in unit time will increase. The effect caused by temperature increasing is determined by the joint action of the above two factors, which can be demonstrated in Figure 4. As shown in Figure 4, for both IgG and BSA, the turning point of biomolecule concentration corresponding to the maximum effect decreases with the temperature rising. Temperature changes will affect the intermolecular collisions, which will change the number of translocation. For two kinds of biomolecules, when the temperature is low, increasing temperature could lead to increasing thermal motion of protein molecules, which can promote protein migration; when the temperature continues to rise, when the molecular collision greatly increases, translocation current will decrease. Consequently, higher temperature will make earlier arrival to the saturation of biomolecules' translocation, which results in the turning point for the maximum shifting to lower concentration for both IgG and BSA.

According to the above discussion, temperature affects the translocation of mainly through the speed of
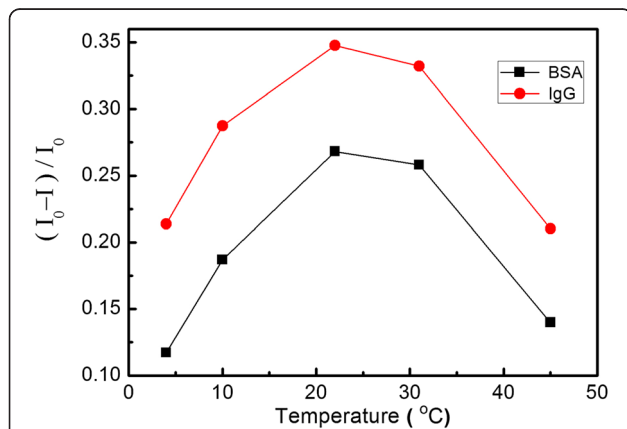

Figure 5 The value of $(I_0 - I)/I_0$ modulated by the viscosity of solution. Biomolecule: IgG, KCl: 0.1 mol/L, temperature: 22°C.

biomolecules and molecular collision between biomolecules. The number of collisions (Z) in local space can be calculated by Equation (2). In order to understand the influence on the translocation by the speed of biomolecules, similar experiments have been carried out (biomolecule: IgG, KCl: 0.1 mol/L, temperature: 22°C), and the difference is certain volume percent of glycerol which was added in the solution. Glycerol can change the viscosity of the solution and influence the speed of biomolecules. Of course, glycerol will also influence the basic ionic current; in our experiment, the detected basic currents are 44.7, 42.8, 40.3, and 35.9 μA when the volume percent of glycerol is 0%, 5%, 10%, and 15%, respectively. From the results shown in Figure 5, it indicates that the turning point for the maximum value of

Figure 4 The value of $(I_0 - I)/I_0$ modulated by temperature. The electrolyte concentration is fixed at 0.01 mol/L, and protein concentration is fixed at 40 ng/L.
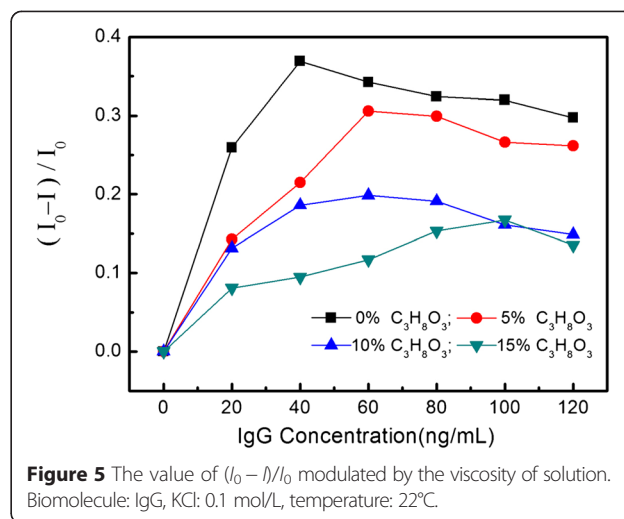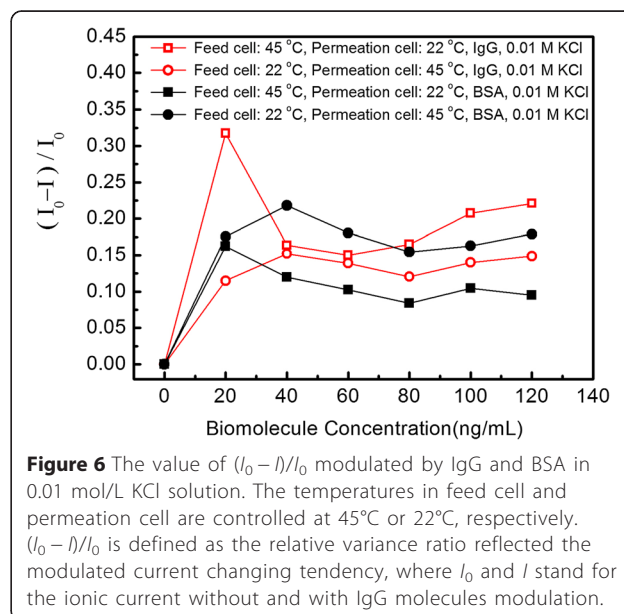

Figure 6 The value of $(I_0 - I)/I_0$ modulated by IgG and BSA in 0.01 mol/L KCl solution. The temperatures in feed cell and permeation cell are controlled at 45°C or 22°C, respectively. $(I_0 - I)/I_0$ is defined as the relative variance ratio reflected the modulated current changing tendency, where I_0 and I stand for the ionic current without and with IgG molecules modulation.

$(I_0 - I)/I_0$ shifts to bigger biomolecule concentrations, which mainly determined by the IgG speed decrease resulted from the viscosity increase of the solution.

In above discussion, the capture probability of IgG molecule which mainly influences biomolecule translocations and ionic currents is discussed in the region nearby nanopore on the side of feed cell. Once IgG or BSA molecule is captured by nanopore, it will move to the permeation cell under the strong voltage drop and then leave nanopore on the side of permeation cell rapidly after its translocation. So the turning point for the maximum $(I_0 - I)/I_0$ value is mainly defined by the temperature in the feed cell, which is supported by the experimental results obtained in temperature difference conditions. As shown in Figure 6, if the temperatures are controlled at 45°C in feed cell and 22°C in permeation cell, the turning point for IgG and BSA is similar to the case with the temperatures being controlled at 45°C in both cells. Conversely, if the temperatures are controlled at 22°C in feed cell and 45°C in permeation cell, the turning point for IgG and BSA is similar to the case with the temperatures being controlled at 22°C in both cells.

Conclusions

In summary, the thermally controlled biomolecular transport properties have been investigated by a nanofluidic device with a feed cell and a permeation cell linked by a chip containing nanopores arrays. The results indicate that there exists a maximum decreasing value in each modulated current curve with biomolecule concentration increasing because of the thermally induced intermolecular collision, which is mainly influenced by the temperature in feed cell.

Competing interests
The authors declare that they have no competing interests.

Authors' contributions
LL carried out the experimental design and result analysis and part of the experimental work and drafted the manuscript. LZ carried out part of the experimental work. Both authors read and approved the final manuscript.

References
1. Qiu XY, Yu HZ, Karunakaran M, Pradeep N, Nunes SP, Peinemann KV. Selective separation of similarly sized proteins with tunable nanoporous block copolymer membranes. ACS Nano. 2013;7:768–76.
2. Li XF, Fustin CA, Lefevre N, Gohy JF, De Feyter S, De Baerdemaeker J, et al. Ordered nanoporous membranes based on diblock copolymers with high chemical stability and tunable separation properties. J Mater Chem. 2010;20:4333–9.
3. Gu LQ, Ritzo B, Wang Y. Biosensing: when less is more in a nanopore. Nat Nanotech. 2012;7:212–3.
4. Kant K, Yu JX, Priest C, Shapter JG, Losic D. Impedance nanopore biosensor: influence of pore dimensions on biosensing performance. Analyst. 2014;139:1134–40.
5. Guo W, Cao L, Xia J, Nie FQ, Ma W, Xue J, et al. Energy harvesting with single-ion-selective nanopores: a concentration-gradient-driven nanofluidic power source. Adv Funct Mater. 2010;20:1339–44.
6. Cervera J, Ramirez P, Mafe S, Stroeve P. Asymmetric nanopore rectification for ion pumping, electrical power generation, and information processing applications. Electrochim Acta. 2011;56:4504–11.
7. Kim ES, Jang DS, Yang SY, Lee MN, Jin KS, Cha HJ, et al. Controlled release of human growth hormone fused with a human hybrid Fc fragment through a nanoporous polymer membrane. Nanoscale. 2013;5:4262–9.
8. Zharov I, Khabibullin A. Surface-modified silica colloidal crystals: nanoporous films and membranes with controlled ionic and molecular transport. Acc Chem Res. 2014;47:440–9.
9. Jeon G, Yang SY, Kim JK. Functional nanoporous membranes for drug delivery. J Mater Chem. 2012;22:14814–34.
10. Jackson EA, Hillmyer MA. Nanoporous membranes derived from block copolymers: from drug delivery to water filtration. ACS Nano. 2010;4:3548–53.
11. Schoch RB, Han J, Renaud P. Transport phenomena in nanofluidics. Rev Mod Phys. 2008;80:839–83.
12. Nam SW, Rooks MJ, Kim KB, Rossnagel SM. Ionic field effect transistors with sub-10 nm multiple nanopores. Nano Lett. 2009;9:2044–8.
13. Guan W, Fan R, Reed MA. Field-effect reconfigurable nanofluidic ionic diodes. Nat Commun. 2011;2:506.
14. Perry JM, Zhou K, Harms ZD, Jacobson SC. Ion transport in nanofluidic funnels. ACS Nano. 2010;4:3897–902.
15. Bayley H, Cremer PS. Stochastic sensors inspired by biology. Nature. 2001;413:226–30.
16. Bayley H, Jayasinghe L. Functional engineered channels and pores - (Review). Mol Membr Biol. 2004;21:209–20.
17. Wanunu M, Bhattacharya S, Xie Y, Tor Y, Aksimentiev A, Drndic M. Nanopore analysis of individual RNA/antibiotic complexes. ACS Nano. 2011;5:9345–53.
18. Chang H, Kosari F, Andreadakis G. DNA-mediated fluctuations in ionic current through silicon oxide nanopore channels. Nano Lett. 2004;4:1551–6.
19. Lee MH, Lee JH, Kim HM, Kim YR, Jeon TJ, Pak YE, et al. Leakage current in a Si-based nanopore structure and its influence on noise characteristics. Microfluid Nanofluidics. 2014;16:123–30.
20. Siwy Z, Apel P, Baur D, Dobrev DD, Korchev YE, Neumann R, et al. Preparation of synthetic nanopores with transport properties analogous to biological channels. Surf Sci. 2003;532:1061–6.
21. Harrell CC, Choi Y, Horne LP, Baker LA, Siwy ZS, Martin CR. Resistive-pulse DNA detection with a conical nanopore sensor. Langmuir. 2006;22:10837–43.
22. Mara A, Siwy Z, Trautmann C, Wan J, Kamme F. An asymmetric polymer nanopore for single molecule detection. Nano Lett. 2004;4:497–501.
23. Avdoshenko SM, Nozaki D, da Rocha CG, Gonzalez JW, Lee MH, Gutierrez R, et al. Dynamic and electronic transport properties of DNA translocation through graphene nanopores. Nano Lett. 2013;13:1969–76.
24. Li CY, Ma FX, Wu ZQ, Gao HL, Shao WT, Wang K, et al. Solution-pH-modulated rectification of ionic current in highly ordered nanochannel arrays patterned with chemical functional groups at designed positions. Adv Funct Mater. 2013;23:3836–44.
25. Sparreboom W, van den Berg A, Eijkel JCT. Principles and applications of nanofluidic transport. Nat Nanotechnol. 2009;4:713–20.
26. Hou X, Guo W, Jiang L. Biomimetic smart nanopores and nanochannels. Chem Soc Rev. 2011;40:2385–401.
27. Hummer G, Rasaiah JC, Noworyta JP. Water conduction through the hydrophobic channel of a carbon nanotube. Nature. 2001;414:188–90.
28. Majumder M, Chopra N, Andrews R, Hinds B. Nanoscale hydrodynamics - enhanced flow in carbon nanotubes. Nature. 2005;438:44–4.
29. Chinen H, Mawatari K, Pihosh Y, Morikawa K, Kazoe Y, Tsukahara T, et al. Enhancement of proton mobility in extended-nanospace channels. Angew Chem Int Ed. 2012;51:3573–7.

30. Wei R, Gatterdam V, Wieneke R, Tampe R, Rant U. Stochastic sensing of proteins with receptor-modified solid-state nanopores. Nat Nanotechnol. 2012;7:257–63.

31. Striemer CC, Gaborski TR, McGrath JL, Fauchet PM. Charge- and size-based separation of macromolecules using ultrathin silicon membranes. Nature. 2007;455:749–53.

32. Jirage KB, Hulteen JC, Martin CR. Nanotubule-based molecular-filtration membranes. Science. 1997;278:655–8.